

# Correspondence

## Multiscale Image Fusion Using Complex Extensions of EMD

David Looney and Danilo P. Mandic

**Abstract**—Empirical mode decomposition (EMD) is a fully data driven technique for decomposing signals into their natural scale components. However the problem of uniqueness, caused by the empirical nature of the algorithm and its sensitivity to changes in parameters, makes it difficult to perform fusion of data from multiple and heterogeneous sources. A solution to this problem is proposed using recent complex extensions of EMD which guarantees the same number of decomposition levels, that is the uniqueness of the scales. The methodology is used to address multifocus image fusion, whereby two or more partially defocused images are combined in automatic fashion so as to create an all in focus image.

**Index Terms**—Complex-valued signal processing, empirical mode decomposition (EMD), image fusion.

### I. INTRODUCTION

A significant challenge in data and information fusion is the fusion of images with different focus points so as to create an all-in-focus image. This is of particular importance, for example, in modern microscopy where the resolution is compromised by the limited depth of focus. Existing solutions [1], [2] are based on the assumptions that data exhibit some structure (linearity, sparsity), and on the subsequent applications of projections onto a set of predefined basis functions. For instance principal component analysis (PCA), commonly used for image fusion [3], is based on linear projections and is hence suboptimal for real-world data. Other established solutions include the wavelet transform [4], which experiences problems (by design) when analyzing high-frequency content, thus tending to lose spatial information.

The recently proposed empirical mode decomposition EMD [5] is a fully data driven technique which decomposes the signal into narrow-band oscillatory components called intrinsic mode functions (IMFs). Unlike Fourier or wavelet based methods that project signals onto a fixed basis set, EMD makes no prior assumptions about the data and as such it belongs to the class of exploratory data analysis techniques [6]. The original algorithm has been successfully applied to a number of problems which require high resolution but are separable in the time-frequency domain, such as in ocean engineering [7], biomedical signal processing [8] and seismics [9].

Recently, EMD has been proposed for data fusion, within the so-called “information fusion via fission” framework [10], whereby only the “relevant” IMFs are recombined into a restored signal. The potential of EMD in this context has been demonstrated by a variety of related tasks from signal restoration [11] to feature extraction [12]. Considering its ability to separate spatial frequencies, it is natural to consider EMD for the problem of heterogeneous image fusion.

Manuscript received April 29, 2008; revised October 30, 2008. First published January 09, 2009; current version published March 11, 2009. The associate editor coordinating the review of this manuscript and approving it for publication was Dr. Mark J. Coates.

The authors are with the Imperial College London, London SW7 2BT, U.K. (e-mail: david.looney06@imperial.ac.uk; d.mandic@imperial.ac.uk).

Digital Object Identifier 10.1109/TSP.2008.2011836

A significant obstacle to heterogeneous fusion applications, however, is the problem of uniqueness within EMD. That is there is no guarantee that decompositions of different sources are matched, either in number or their properties (frequency), making a multiscale comparison often very difficult. Thus, a set of common frequency scales must be determined in order to facilitate multiscale image fusion.

In [13], the use of EMD was proposed for the fusion of visual and thermal images, it was shown how EMD outperformed wavelet and PCA based approaches, particularly in retaining edge-based information from the different image modalities. Although aided by a mutual information measure, the approach [13] revealed the difficulties in combining IMFs from heterogeneous sources as it relied on visual inspection to determine the most informative components. More recent work [14] considers a 2-D (two-dimensional) extension for the related task of multispectral image fusion. Although fusion is performed in an automatic fashion, the solution does not address the problem of uniqueness.

In this correspondence we propose to use recent complex extensions of EMD [15], [16], originally designed for naturally bivariate or complex signals, to circumvent the problem of uniqueness. This makes it possible to perform heterogeneous image fusion based on the common spatio-temporal scales.

### II. THE EMD ALGORITHM

Empirical mode decomposition [5] is a data driven time-frequency technique which adaptively decomposes a signal, by means of a process called the sifting algorithm, into a finite set of AM/FM modulated components. These components, called “intrinsic mode functions” (IMFs), represent the oscillation modes embedded in the data. By definition, an IMF is a function for which the number of extrema and the number of zero crossings differ by at most one, and the mean of the two envelopes associated with the local maxima and local minima is approximately zero. The EMD algorithm decomposes the signal  $x(k)$  as

$$x(k) = \sum_{i=1}^M C_i(k) + C_r(k) \quad (1)$$

where  $C_i(k)$ ,  $i = 1, \dots, M$ , are the IMFs and  $C_r(k)$  is the residue. The first IMF is obtained as follows [5].

- 1) Let  $\tilde{x}(k) = x(k)$ .
- 2) Identify all local maxima and minima of  $\tilde{x}(k)$ .
- 3) Find an “envelope,”  $e_{\min}(k)$  (respectively  $e_{\max}(k)$ ) that interpolates all local minima (respectively maxima).
- 4) Extract the “detail,”  $d(k) = x(k) - (1/2)(e_{\min}(k) + e_{\max}(k))$ .
- 5) Let  $\tilde{x}(k) = d(k)$  and go to step 2); repeat until  $d(k)$  becomes an IMF.

Once the first IMF is obtained, the procedure is applied iteratively to the residual  $r(k) = x(k) - d(k)$  to obtain all the IMFs.

For notational convenience, in the sequel the residue is included as the last IMF, that is,  $C_M(k) = C_r(k)$ .

### III. FUSION OF HETEROGENEOUS SOURCES

In theory, it is natural to consider EMD for fusion due to its ability to separate spatial frequencies in an adaptive way. However, because it is fully data-driven, it is unlikely that matching IMFs will be produced for heterogeneous sources. Thus, making fusion difficult. Furthermore,

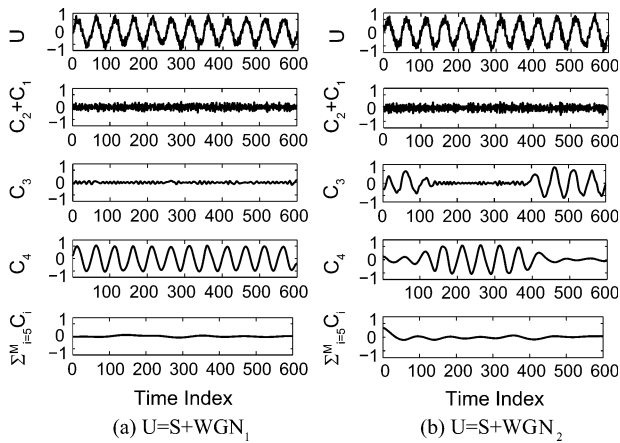


Fig. 1. Real EMD: Signals with similar statistics often produce IMFs that are different in number [ $M = 8$  for (a) and  $M = 9$  for (b)] and frequency [note the mode-mixing in (b)].

the local operation of EMD makes it sensitive to changes in parameters (stopping criterion, choice of interpolation) and also to local signal variations caused by added noise [17]. In short, its local and data-driven nature cause two significant problems:

- 1) uniqueness of the decomposition—signals, even with similar statistics, give different IMFs;
- 2) mode-mixing—the phenomenon whereby similar modes appear across different frequency scales.

To illustrate these problems, consider a sinusoid  $\mathbf{S}$  with added white Gaussian noise (AWGN), denoted by  $\mathbf{U}$  in the top panel of Fig. 1(a). Fig. 1(a) also shows the eight extracted IMFs where, for convenience, the lower panel denotes  $\sum_{i=5}^M C_i = C_5 + C_6 + C_7 + C_8$ . Observe that the original noise-free sinusoid corresponds to the fourth IMF and that a standard way of applying EMD (denoising) would be to retain this component and omit the rest. Performing EMD on the same sinusoid corrupted by a different realization of AWGN, but with the same statistics as before (mean, variance), nine IMFs were obtained, as shown in Fig. 1(b). In addition to a different number of IMFs (uniqueness), the signal of interest is now spread across different scales ( $C_3$  and  $C_4$ ) illustrating mode-mixing. Therefore, even though the statistical (global) properties of the signal remain the same, the difference in local properties have affected the decomposition.

The problem of uniqueness can be addressed by stopping the decomposition once a given number of IMFs have been obtained, however, this is suboptimal as a guarantee on the number of IMFs is only a necessary requirement which does not uniquely facilitate that the decomposition properties are matched. One solution for mode-mixing is Ensemble EMD [17], however this does not solve the uniqueness problem and is further limited by its computational complexity. To use EMD for data fusion, the following problems have to be addressed:

- the number of IMFs from each source must be equal;
- the IMF properties from each source should also be matched to enable a meaningful comparison.

To this end, we propose to apply recent complex extensions of the EMD algorithm [15], [16], [18] so as to decompose data from heterogeneous sources simultaneously. We illustrate that this guarantees the IMFs are matched in number and properties, thus finding a set of common scales which are unique to the sources being analyzed and facilitating fusion.

#### IV. COMPLEX EXTENSIONS OF EMD

Several extensions of EMD have been recently developed. These include “complex empirical mode decomposition” [18], “rotation in-

variant empirical mode decomposition” [15] and “bivariate empirical mode decomposition” [16].

Complex EMD is derived from the inherent relationship between the positive and negative frequency components of a complex signal and the properties of the Hilbert transform. The idea behind this approach is rather intuitive: first note that a complex signal has a two-sided, asymmetric spectrum. The complex signal can therefore be converted into a sum of analytic signals by a straightforward filtering operation that extracts the opposite sides of the spectrum. Direct analysis in  $\mathbb{C}$  can subsequently be achieved by applying standard EMD to both the positive and negative frequency parts of the signal. Although it retains important properties of univariate EMD, such as its behavior as a dyadic filter bank, it is difficult to interpret the meaning of extracted IMFs and the approach is not suitable for extensions to higher dimensions.

The rotation invariant EMD (RIEMD) operates completely within  $\mathbb{C}$  based on the direct application of complex splines. The complex envelope approximation is characterized by the definition of suitable extrema in  $\mathbb{C}$ . This is not straightforward since  $\mathbb{C}$  is not an ordered field [10], and RIEMD defines an extrema as a locus where the angle of the complex-valued first derivative becomes zero, that is, it is based on a change in the phase of the signal. This definition is equivalent to the extrema of the imaginary part, that is, for a complex signal  $Z(t)$  (for convenience a continuous time index  $t$  is used)

$$\begin{aligned} \angle \dot{Z}(t) = 0 &\Rightarrow \angle \{\dot{x}(t) + j \cdot \dot{y}(t)\} = 0 \\ &\Rightarrow \tan^{-1} \frac{\dot{y}(t)}{\dot{x}(t)} = 0 \Rightarrow \dot{y}(t) = 0. \end{aligned} \quad (2)$$

Unlike complex EMD, the IMFs of rotation invariant EMD possess a physical meaning as is illustrated by its analysis of real-world complex quantities such as wind data [15].

Bivariate EMD [16] operates in a similar fashion to rotation invariant EMD. By projecting the data in  $k$  directions, the approach can consider extrema in several directions and construct a 3-D tube to enclose them. The local mean is defined as the center of the tube which is described, at each interval, by  $k$  points (with each point being associated with a specific direction). Assuming  $k = 4$  directions, the center of the tube at a point is given by either the barycenter of the four points or the intersection of straight lines passing through the middle of the tangents. RIEMD and bivariate EMD are equivalent for the case of  $k = 2$ . Both algorithms operate fully in  $\mathbb{C}$ , generating an equal number of IMFs for the real and imaginary components, thus making it possible to analyze two-dimensional data.

Since bivariate EMD can operate for  $k > 2$ , this method was used for simulations using  $k = 8$  directions and defining the center of the 3-D tube as the intersection of straight lines passing through the middle of the tangents.

#### V. MULTISCALE FUSION VIA EMD

We propose to regard data from multiple sources as a single multidimensional entity which, for two sources, facilitates the use of a complex extension of EMD (either [15] or [16]). Under the assumption that the analysis determines common oscillations on a scale by scale level, the source which contains locally the most information can be determined by performing a comparison between the real and imaginary components of the IMFs. One suitable feature choice is local changes in the variance of the IMFs, as shown in [14].

For rigor, simulations were initially performed on artificially generated data sets so as to illustrate its potential in finding “common data scales.” Next, an automatic fusion algorithm is proposed and applied to a real-world fusion problem, creating an all-in-focus image from images which are partially out of focus.

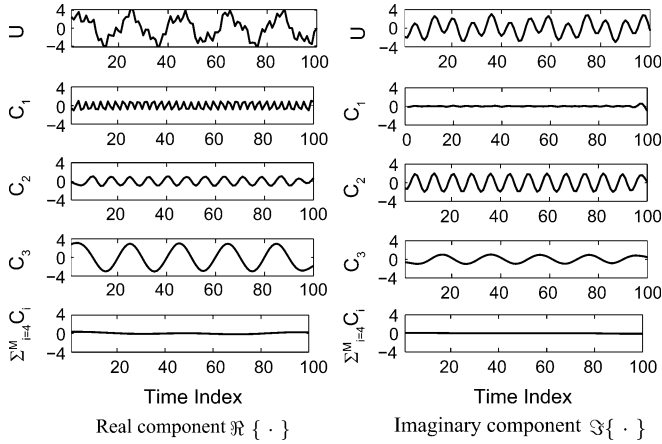


Fig. 2. Simultaneous decomposition of two test signals ( $\Re\{U\}$  and  $\Im\{U\}$ ) using bivariate EMD gives matched scales, highlighting its ability to find common scales in heterogeneous sources.

#### A. Test Sets

In the first experiment, two signals were constructed from a set of three sinusoidal components. These signals are visible in the top panels (denoted by  $\Re\{U\}$  and  $\Im\{U\}$ ) of Fig. 2. Common to each test signal were the frequencies of two of the sinusoids, although their amplitudes and phases were different. A third high-frequency sinusoid was added to  $\Re\{U\}$  only. Performing bivariate EMD on the complex signal constructed from each of these signals ( $\Re\{U\} + j\Im\{U\}$ ), a set of complex IMFs were obtained, for which the real and imaginary values of which are shown in Fig. 2.

Observe the high-frequency sinusoid, contained only within  $\Re\{U\}$ , in the real part of the first IMF. On the other hand, the imaginary component,  $\Im\{C_1\}$ , shows comparatively less high-frequency content. The methodology can determine, however, common frequency scales as is evident by comparing  $\Re\{C_2\}$  and  $\Im\{C_2\}$  as well as  $\Re\{C_3\}$  and  $\Im\{C_3\}$ . Note that the approach is robust to changes in scale amplitude as well as phase, thus solving the problem of uniqueness.

In the next experiment, bivariate EMD was performed on a complex signal, the real and imaginary components of which are shown respectively in the top panels (denoted by  $\Re\{U\}$  and  $\Im\{U\}$ ) of Fig. 3. The real component was a sinusoid corrupted by AWGN. The imaginary component was the same sinusoid, shifted by an arbitrary phase value and with its amplitude reduced by a factor of 2, corrupted by different AWGN but with the same statistics as the AWGN affecting the real component. The set of complex IMFs are shown componentwise in Fig. 3.

Note that most of the noise is contained within the first three IMFs and the signal of interest (sinusoid) is spread across subsequent IMF components. This result demonstrates that although the approach can be affected by the problem of mode-mixing, it is irrelevant as it occurs simultaneously in each channel as indicated by components  $C_4$  and  $C_5$ . Simulations with higher noise (up to 2.6 dB) support these results. Thus, its robustness guarantees a meaningful comparison between scales and forms the basis for the proposed image fusion algorithm.

#### B. Multi-Scale Image Fusion

Simultaneous decomposition of two partially defocused images, A and B, is proposed as follows. The rows of each of the images are concatenated so as to construct two vectors ( $v_1$  and  $v_2$ ) and, using bivariate EMD, the complex vector  $v_1 + jv_2$  is decomposed into  $M$  complex

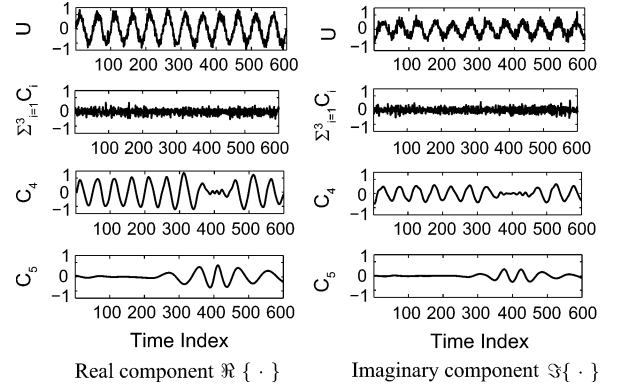


Fig. 3. Simultaneous decomposition of two test signals ( $\Re\{U\}$  and  $\Im\{U\}$ ) using bivariate EMD, highlighting its robustness to mode mixing as it occurs simultaneously ( $C_4$  and  $C_5$ ).

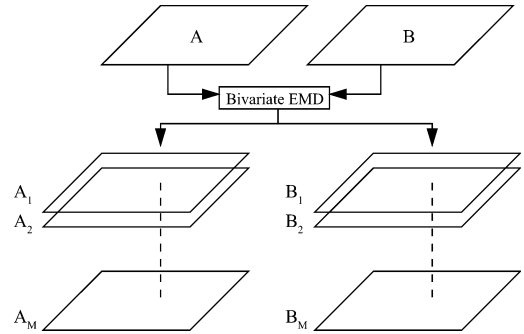


Fig. 4. Proposed framework for the simultaneous decomposition of two images.

IMFs.<sup>1</sup> Separating the IMFs into their real and imaginary components and reconverting each into their original 2-D form gives a set of  $M$  scale images for both A and B, denoted by  $A_i$  and  $B_i$  for  $i = 1, \dots, M$ . This is illustrated in Fig. 4.

The fused image,  $F$ , is then given by

$$F(x, y) = \sum_{i=1}^M [\alpha_i(x, y)A_i(x, y) + \beta_i(x, y)B_i(x, y)] \quad (3)$$

where  $(x, y)$  denotes the spatial location in the image and  $\alpha_i(x, y)$  and  $\beta_i(x, y)$  are weighted coefficients which satisfy  $\alpha_i(x, y) + \beta_i(x, y) = 1$ . The values for the coefficients are determined by comparing the local variance for each scale at each location as

$$\begin{aligned} \alpha_i(x, y) &= 0 \text{ if } \text{var}\{A_i(x, y)\} - \text{var}\{B_i(x, y)\} < -\epsilon \\ \alpha_i(x, y) &= 0.5 \text{ if } |\text{var}\{A_i(x, y)\} - \text{var}\{B_i(x, y)\}| < \epsilon \\ \alpha_i(x, y) &= 1 \text{ if } \text{var}\{A_i(x, y)\} - \text{var}\{B_i(x, y)\} > \epsilon \end{aligned} \quad (4)$$

where  $\epsilon > 0$  and where  $\text{var}\{A_i(x, y)\}$  denotes the local variance at  $(x, y)$  for  $A_i$ , that is

$$\text{var}\{A_i(x, y)\} = \sum_{m=-N_i}^{N_i} \sum_{n=-N_i}^{N_i} [A_i(x+m, y+n) - \mu]^2 \quad (5)$$

<sup>1</sup>It was found that the addition of low level white Gaussian noise to the real and imaginary components, prior to their decomposition using bivariate EMD, facilitated a more natural separation of the scale components. For more detail we refer to [17].

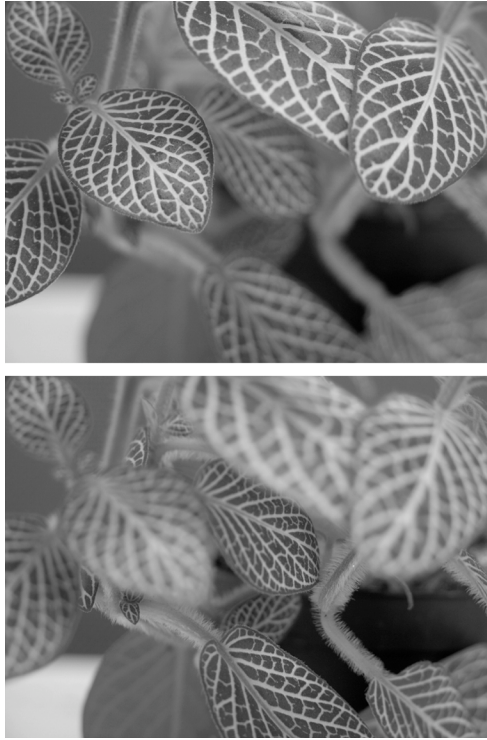


Fig. 5. Partially defocused images. Top: Foreground focus. Bottom: Background focus.

where  $\mu$  is the mean of all the elements contained within the window and  $N_i$  determines the window size. An advantage of the proposed approach is that  $N_i$  can be increased as  $i$  increases to better accommodate scale images with lower spatial information. Thus, the fused image retains locally dominant features (in this case determined by local variance) at each scale.

An added obstacle in applying a 1-D algorithm to an image is caused by its inherent 2-D structure. Consequently, some information is lost in the vertical direction (if the rows are concatenated) which can cause horizontal artifacts in the scale images. In general, it was found that any such artifacts in the high-frequency scales were not significant. However, in some cases, it was found that the loss in structure of the lower scales became more pronounced. To circumvent this problem, the scales with sufficiently low frequencies are added together to form a composite residue scale image which was found to have greater structure than the individual low-frequency scale images. This way, the fusion algorithm described above is performed on an alternate set of  $M' < M$  scale images,  $A'$  and  $B'$ , given by

$$A'_i = \begin{cases} A_i & \text{for } i = 1, \dots, M' - 1 \\ \sum_{q=M'}^M A_q & \text{for } i = M' \end{cases}$$

$$B'_i = \begin{cases} B_i & \text{for } i = 1, \dots, M' - 1 \\ \sum_{q=M'}^M B_q & \text{for } i = M'. \end{cases}$$

if  $f(A_{M'-1}, B_{M'-1}) < \delta$  where  $f(\cdot)$  is an operator which determines the average spatial frequencies of the scale images and  $\delta$  is an appropriate threshold.

In the next experiment, the proposed methodology was applied to the images shown in Fig. 5. Observe the sharp edges and high level of detail in the focused region of each image. This is a realistic situation as the

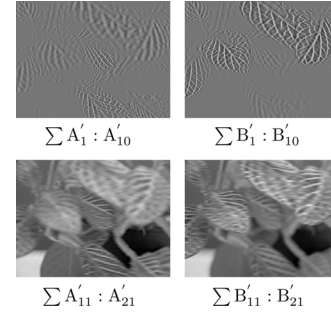


Fig. 6. Scale images for Fig. 5. Different spatial information is contained in the scales such as edge information (high-frequency scales) and illumination information (low-frequency scales).

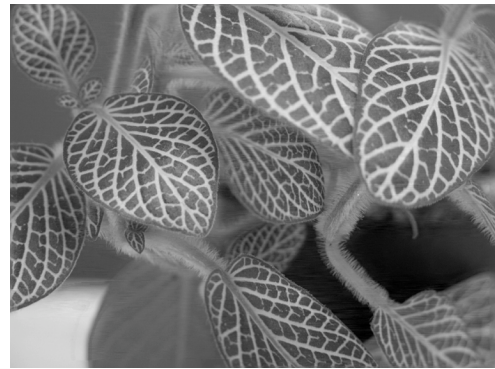


Fig. 7. All-in-focus image obtained by bivariate EMD.

focused regions are located in a random fashion. Setting  $\delta = 0.01 \times \mathbf{Fs}$ , where  $\mathbf{Fs}$  denotes the image sampling frequency, a set of  $M' = 21$  scale images were obtained which are shown in Fig. 6. Observe that the image edge information is contained in the high-frequency scales and that illumination effects are contained in the low scales. Fusion of the partially defocused images is shown in Fig. 7. As desired, the fused image retains all the detail of the original images and any spurious fusion artifacts are kept to a minimum.

The application of complex extensions of EMD to image fusion clearly illustrates that they overcome the problems of mode-mixing and uniqueness. Higher dimensional extensions should be developed to facilitate the fusion of more than two images, a subject of our future work.

## VI. CONCLUSION

The potential of complex extensions of empirical mode decomposition (EMD) for information fusion has been verified. The analysis has shown that a set of common frequency scales can be determined by simultaneously decomposing sources using the bivariate EMD. This enables the proposed approach to overcome the problems of uniqueness and mode-mixing, major obstacles to EMD-based fusion. The benefits of the proposed framework have been demonstrated by simulations both on test sets and real-world images.

## REFERENCES

- [1] T. Stathaki, *Image Fusion: Algorithms and Applications*. New York: Academic, 2008.
- [2] C. Pohl and J. L. Van Genderen, "Multisensor image fusion in remote sensing: Concepts, methods and applications," *Int. J. Remote Sens.*, vol. 19, no. 5, pp. 823–854, 1998.

- [3] H. Yesou, Y. Besnus, and J. Rolet, "Extraction of spectral information from landsat TM data and merger with SPOT panchromatic imagery—A contribution to the study of geological structures," *ISPRS J. Photogrammetry Remote Sens.*, vol. 48, no. 5, pp. 23–36, 1993.
- [4] H. Li, B. S. Manjunathand, and S. K. Mitra, "Multisensor image fusion using the wavelet transform," *Graph. Models Image Process.*, vol. 57, no. 3, pp. 235–245, 1995.
- [5] N. E. Huang, Z. Shen, S. R. Long, M. L. Wu, H. H. Shih, Z. Quanan, N. C. Yen, C. C. Tung, and H. H. Liu, "The empirical mode decomposition and the Hilbert spectrum for nonlinear and non-stationary time series analysis," *Proc. Roy. Soc. A*, vol. 454, pp. 903–995, 1998.
- [6] J. W. Tukey, *Exploratory Data Analysis*. Reading, MA: Addison-Wesley, 1977.
- [7] M. Datig and T. Schlurmann, "Performance and limitations of the Hilbert-Huang Transformation (HHT) with an application to irregular water waves," *Ocean Eng.*, vol. 31, pp. 1783–1834, Oct. 2004.
- [8] T. M. Rutkowski, R. Zdunek, and A. Cichocki, "Multichannel EEG brain activity pattern analysis in time-frequency domain with nonnegative matrix factorization support," in *Int. Congr. Series*, 2007, vol. 1301, pp. 266–269.
- [9] R. R. Zhang, S. Ma, E. Safak, and S. Hartzell, "Hilbert-Huang transform analysis of dynamic and earthquake motion recordings," *J. Eng. Mech.*, vol. 129, pp. 861–875, 2003.
- [10] D. P. Mandic, M. Golz, A. Kuh, D. Obradovic, and T. Tanaka, *Signal Processing Techniques for Knowledge Extraction and Information Fusion*. New York: Springer, 2008.
- [11] D. Looney and D. P. Mandic, "A machine learning enhanced empirical mode decomposition," in *Proc. Int. Conf. Acoustics, Speech, Signal Processing (ICASSP)*, 2008, pp. 1897–1900.
- [12] D. Looney, L. Li, T. Rutkowski, D. P. Mandic, and A. Cichocki, "Ocular artifacts removal from EEG using EMD," presented at the 1st Int. Conf. Cognitive Neurodynamics, Shanghai, China, Nov. 2007.
- [13] H. Hariharan, A. Gribok, M. A. Abidi, and A. Koschan, "Image fusion and enhancement via empirical mode decomposition," *J. Pattern Recognit. Res. (JPRR)*, vol. 1, no. 1, pp. 16–32, 2006.
- [14] X. Xu, H. Li, and A. N. Wang, "The application of BEMD to multi-spectral image fusion," in *Proc. Int. Conf. Wavelet Analysis Pattern Recognition (ICWAPR)*, 2007, vol. 1, pp. 448–452.
- [15] M. U. B. Altaf, T. Gautama, T. Tanaka, and D. P. Mandic, "Rotation invariant complex empirical mode decomposition," in *Proc. Int. Conf. Acoustics, Speech, Signal Processing (ICASSP)*, 2007, vol. 3, pp. 1009–1012.
- [16] G. Rilling, P. Flandrin, P. Goncalves, and J. M. Lilly, "Bivariate empirical mode decomposition," *IEEE Signal Process. Lett.*, vol. 14, pp. 936–939, 2007.
- [17] Z. Wu and N. E. Huang, "Ensemble empirical mode decomposition: A noise-assisted data analysis method," Center for Ocean-Land-Atmosphere Studies, Tech. Rep. 193, 2004.
- [18] T. Tanaka and D. P. Mandic, "Complex empirical mode decomposition," *IEEE Signal Process. Lett.*, vol. 14, pp. 101–104, Feb. 2007.

## Semidefinite Programming Approach for Range-Difference Based Source Localization

Kenneth Wing Kin Lui, Frankie Kit Wing Chan, and H. C. So

**Abstract**—A common technique for passive source localization is to utilize the range-difference (RD) measurements between the source and several spatially separated sensors. The RD information defines a set of hyperbolic equations from which the source position can be calculated with the knowledge of the sensor positions. Under the standard assumption of Gaussian distributed RD measurement errors, it is well known that the maximum-likelihood (ML) position estimation is achieved by minimizing a multimodal cost function which corresponds to a difficult task. In this correspondence, we propose to approximate the nonconvex ML optimization by relaxing it to a convex optimization problem using semidefinite programming. A semidefinite relaxation RD-based positioning algorithm, which makes use of the admissible source position information, is proposed and its estimation performance is contrasted with the two-step weighted least squares method and nonlinear least squares estimator as well as Cramér–Rao lower bound.

**Index Terms**—Range-difference measurements, semidefinite programming, source localization, time-delay estimation.

### I. INTRODUCTION

Source localization using measurements from an array of spatially separated sensors has received significant attention in the signal processing literature because of its important applications such as navigation [1], wireless communications [2], telecommunications [3], and sensor networks [4]. A common positioning approach is to use the time-difference-of-arrival (TDOA) measurements, that is, the differences in arrival times between pairs of sensor outputs which receive the radiated signal, assuming that the signal propagation speed is a known constant. Multiplying the TDOA by the propagation speed yields the range-difference (RD) and a hyperbola on which the source must lie can be formed. At least three sensors are needed to uniquely estimate the source position in the two-dimensional (2-D) plane while four or more are required for three-dimensional (3-D) localization, with the use of the knowledge of the sensor array geometry.

Basically, there are two approaches for source localization using the hyperbolic equations constructed from the RD measurements. The first approach is based on the nonlinear least-squares (NLS) framework [5]–[7] where Taylor-series expansion is utilized for linearization and the solution is solved in an iterative manner. Under the standard assumption that the RD measurements are Gaussian distributed, the global minimum of the multimodal NLS cost function corresponds to the maximum-likelihood (ML) position estimate. Although optimum estimation performance can be attained, it requires sufficiently precise initial estimates for the global solution, which indicates the difficulty of this approach because of the possibility of local convergence. The second approach is to reorganize the nonlinear equations into a set of linear equations [8]–[12] by squaring them and introducing an extra variable that is a function of the source position, so that global

Manuscript received August 15, 2008; revised November 02, 2008. First published December 09, 2008; current version published March 11, 2009. The associate editor coordinating the review of this manuscript and approving it for publication was Dr. Shahram Shahbazpanahi. The work described in this paper was supported by a grant from CityU (Project No. 7002132).

The authors are with the Department of Electronic Engineering, City University of Hong Kong, Kowloon, Hong Kong (e-mail: hcso@ee.cityu.edu.hk).

Color versions of one or more of the figures in this paper are available online at <http://ieeexplore.ieee.org>

Digital Object Identifier 10.1109/TSP.2008.2010599